Food Hydrocolloids 154 (2024) 110146

Contents lists available at ScienceDirect

Food Hydrocolloids

journal homepage: www.elsevier.com/locate/foodhyd

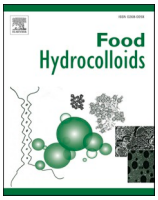

Pickering oil-in-water emulsions stabilized by hybrid plant protein-flavonoid conjugate particles

Nisufyan Nimaming, Amin Sadeghpour, Brent S. Murray, Anwesha Sarkar *

Food Colloids and Bioprocessing Group, School of Food Science and Nutrition, University of Leeds, Leeds, LS2 9JT, United Kingdom

ARTICLE INFO

Keywords:
Potato protein
Quercetin
SAXS
Conjugation
Confocal microscopy
Stability

ABSTRACT

Protein and polyphenols are often found as self-assembled structures in plants. Inspired by nature, this study looked at controlled engineering of hybrid nanoparticles using plant-based proteins and plant-derived flavonoid crystals. These nanoparticles have been shown to stabilize Pickering emulsions over several months. Potato protein (PoP) and flavonoid quercetin (QC) crystals in mass ratios (PoP:QC) ranging from 100:1 to 5:1, were used to fabricate the hybrid (PoPQC) nanoparticles at pH 7.0. The hydrodynamic diameter (d_H), scattering pattern via small angle X-ray scattering (SAXS) and ζ-potential of the PoPQC as well as the protein conformation via circular dichroism (CD) and fluorescence were studied. The oil-in-water (O/W) emulsions stabilized by PoP and PoPQC nanoparticles with degrees of conjugation ranging 0.18–16.55% were analyzed by droplet sizing, ζ-potential measurements, and microscopy across a wide range of length scales. Both CD and SAXS analyses revealed that the conjugation of PoP with QC caused conformational changes in the secondary structure of PoP with the aromatic amino acids interacting with phenolic rings of QC, mainly through hydrophobic interactions. The addition of QC had a considerable impact on both particle size of PoPQC (~50–~400 nm) and consequently the droplet size of the corresponding Pickering emulsions stabilized by these spherical particles ($d_{4,3}$ ~2–~35 μm). The droplet size increased significantly ($p < 0.05$) as the QC content of the particles was increased, whilst the ζ-potential became more negative. Nevertheless, the Pickering emulsions were capable of resisting coalescence over several months, suggesting the application of nature-inspired hybrid nanoparticles.

1. Introduction

Pickering emulsions (PEs) are composed of two immiscible liquids, generally oil-in-water (O/W) or water-in-oil (W/O), stabilized by solid particles, although recently this definition seems to be stretching to include semi-solid and microgel particles as alternatives to classic low molecular weight surfactant emulsifiers. The key feature is that all these particles are effectively irreversibly adsorbed at the oil-water interface due to their high energy of detachment (ΔG_d), whilst also generating significant steric stabilization of droplets by virtue of the particle size, thereby offering ultrastability against coalescence and even Ostwald ripening (Binks, 2002; Dickinson, 2012; Nimaming et al., 2023; Sarkar & Dickinson, 2020). In addition to the growing demand for sustainable and biocompatible sources of Pickering particles, there has been significant interest in the utilization of plant-based proteins for generating such particles. Several plant-based protein particles have been fabricated via various processes and shown to have efficacy in stabilizing emulsions apparently via the Pickering mechanisms, including soy protein nanogels (Chen et al., 2014), soy protein particles (Zheng et al., 2023), pea protein microgels (Zhang & Sarkar, 2020b), gliadin nanoparticles (Peng et al., 2018), peanut protein isolate particles or microgels (Jiao et al., 2018; Wang et al., 2023), potato protein microgels (Aery et al., 2023), and quinoa protein isolate nanoparticles (Qin et al., 2018; Qin and Peng, 2018; Zhang et al., 2021), to name just a few. Nevertheless, the use of single-component particles means that they are often susceptible to disruption by environmental factors such as pH, ionic strength, and temperature, so that the corresponding emulsions can lose the ultrastability (Carpentier et al., 2022; Fu et al., 2019; Hu & Xiong, 2022; Yi et al., 2021; Zhang et al., 2020a; Zhou et al., 2018).

An alternative approach for improving the particle properties is the fabrication of hybrid particles wherein the particle properties are modulated by using a combination of different food-grade materials (Nimaming et al., 2023). Numerous investigations have shown that modification of proteins by complexation with other biopolymeric materials can provide emulsions with higher stability to adverse environmental and biological conditions as well improve other functional

* Corresponding author. Food Colloids and Bioprocessing Group, School of Food Science and Nutrition, University of Leeds, Leeds, LS2 9JT, United Kingdom.
E-mail address: A.Sarkar@leeds.ac.uk (A. Sarkar).

https://doi.org/10.1016/j.foodhyd.2024.110146
Received 27 February 2024; Received in revised form 25 April 2024; Accepted 26 April 2024
Available online 29 April 2024

properties such as resistance to lipid oxidation, dual delivery of encapsulated bioactives, *etc.* (Chang et al., 2022; Dai et al., 2020; Sui et al., 2018; Tavasoli et al., 2022).

In Nature, plant-derived phenolic compounds such as flavonoids tend to co-exist in self-assembly with proteins (Zhang & Wang, 2021b). The self-assembly is a result of mainly non-covalent interactions, *i.e.*, hydrogen bonding and/or hydrophobic interactions, depending on the locations(s) of the hydroxyl group(s) in the flavonoid ring structure (Liu et al., 2022). The polyphenolic residues of such hybrid particles are thought to be largely responsible for any additional benefits of inhibiting oxidative degradation initiated at the interface. The complexation of dairy proteins with polyphenols as hybrid Pickering particles has been investigated (Chen et al., 2023; Li et al., 2021) but conjugation with plant proteins is a relatively new endeavour. A detailed understanding of stabilizing properties of plant protein hybrid particles is complicated by the relative insolubility and high tendency for self-aggregation of the proteins on their own. This study is an attempt to gain such an understanding for a relatively well characterized pair of materials: quercetin (QC) and potato protein (PoP)

PoP has traditionally been considered as a large volume by-product of starch production, whilst more recently it has started to be investigated as a useful functional ingredient by various food manufacturers (Okeudo-Cogan et al., 2024). Given the huge scale of potato cultivation, the transformation of PoP into a more high value-added material would offer major implications for agronomy and the environment. PoP is especially more water-soluble compared to most other plant storage proteins and therefore potentially more useful as a colloidal ingredient (David & Livney, 2016; Edelman et al., 2019; Hu et al., 2021; Kew et al., 2021). PoP is usually categorized into three fractions of total soluble proteins: patatin (40%) with an isoelectric point (IEPs) between pH 4.5 to 5.2, protease inhibitors (50%) with IEPs ranging from pH 5.1–9.0 (Bergmann & Glatter, 2000; Hussain et al., 2021a, Hussain et al., 2021b) and other high molecular weight proteins (10%). The patatin and protease inhibitor have been shown to exhibit antioxidant activities, and they have great foaming and emulsifying properties for delivering bioactive compounds (David & Livney, 2016; Edelman et al., 2019; van Koningsveld et al., 2006; Waglay et al., 2014).

Polyphenols, of which flavonoids are a sub-group, are secondary plant metabolites. Many studies have proposed that they may be beneficial to human health (Ji et al., 2022; Quan et al., 2019). QC is one of the most prevalent dietary flavonoids, composed of three aromatic rings with hydroxyl groups substituting the hydrogen atoms at positions 3, 5, 7, 3′, and 4′-pentahydroxyflavone (Liu et al., 2022), widely distributed in very many plant species and potentially offers diverse biological activities such as anti-inflammatory, anti-cancer, and antioxidant effects. However, its physicochemical instability and insolubility in water reduce its bioavailability and pose a significant barrier to the utilization of QC in functional nutraceutical products or foods in general (Fang et al., 2011; Ji et al., 2022; Liang et al., 2021; Liao et al., 2022; Ma et al., 2021). Complex formation with a protein such as PoP can be a strategy to deliver QC, whilst also creating hybrid particles for Pickering stabilization of emulsion droplets where QC alone is apparently not as effective (Zembyla et al., 2019), at same time retaining the anti-oxidant properties of both components.

Hence, the objective of this study is to investigate the fabrication of hybrid particles composed of PoP and QC and understand their efficiency as Pickering stabilizers compared to conventional emulsions stabilized by PoP molecules alone. The hybrid particles were examined in terms of their physicochemical characteristics, protein conformational changes and their morphology across various length scales via microscopy and small angle X-ray scattering (SAXS). The stability of Pickering emulsions stabilized by hybrid PoPQC particles was examined over 6 months via measurements of particle size and ζ-potential, microscopy at multiple lengthscales.

2. Materials and methods

2.1. Materials

PoP powder was purchased from Henley Bridge (Lewes, UK) containing 90.5% protein, with patatin as the main protein according to Kew et al. (2021). HEPES buffer (2-(4-(2-hydroxyethyl)-1-piperazinyl)-ethanesulfonic acid) was purchased from PanReac AppliChem, ITW Reagents, UK. Quercetin hydrate, a yellow-coloured powder, was purchased from Fluorochem, Hadfield, UK. The solvents used were of analytical grade. Milli-Q water with a resistivity of 18.2 MΩ cm at 25 °C (Millipore Corp., Bedford, UK) was used for preparation of the HEPES buffer and 0.1 M hydrochloric acid (HCl) or sodium hydroxide (NaOH) was used to adjust the pH of the solutions to pH 7.0. Sodium azide (SigmaAldrich, UK) at 0.02 wt% was employed as an antimicrobial agent.

2.2. Preparation of potato protein (PoP) solutions and hybrid potato protein-quercetin (PoPQC) particles

PoP solution at 5.0 wt% was prepared as described previously by Kew et al. (2021), i.e., by dispersing PoP powder in 20 mM HEPES buffer (at pH 7.0) and stirring continuously for 2 h. The solution was centrifuged at 5000 rpm for 15 min and then the supernatant was collected and used as the useable PoP. A stock solution of QC was prepared by dissoving QC crystals at 1.0 wt% concentration in pure ethanol. For hybrid particle fabrication, different volumes of QC stock solution were added slowly to 5.0 wt% PoP to give different mass ratios of PoP: QC, namely 100: 1, 20: 1, 10: 1, 10: 1.5, and 5: 1 (w/w) at pH 7.0 under the magnetic stirring. The corresponding PoP/QC molar ratios were 0.13, 0.66, 1.32, 1.99, and 2.65, respectively where molar mass of PoP was taken from patatin. The ethanol was then evaporated, re-preciptating the QC in the presence of the PoP and the hybrid particles formed (PoPQC) are subsequently referred to as PoPQC100: 1, PoPQC20: 1, PoPQC10: 1, PoPQC10: 1.5, and PoPQC5: 1, respectively.

2.3. Characterization of hybrid PoPQC particles

2.3.1. Dynamic light scattering

The mean hydrodynamic diameter (d_H) of the PoP and PoPQC dispersions at pH 7.0 was measured by dynamic light scattering (DLS) at 25 °C using a Malven Zetasizer Nano-ZS (Malvern Instruments, Malvern, UK) using a standard disposable cuvette. The absorption coefficient of the PoP and hybrid particles (PoPQC) was set as 0.001. These samples were diluted to 1 mg/mL with Milli-Q water (pH 7.0) and the mean value of d_H, particle size distribution (PSD), and polydispersity index (PDI) were reported.

2.3.2. ζ-potential measurements

A particle electrophoresis instrument (Zetasizer, Nano ZS series, Malvern Instruments, Worcestershire, UK) was used to determine the ζ-potential of PoP, PoPQC and the corresponding emulsions. The PoP and PoPQC samples were diluted to 0.1 mg/mL and the emulsions were diluted to 0.01 wt% oil with Milli-Q water and then fed to a folded capillary cell (Model DTS 1070, Malvern Instruments Ltd., Worcestershire, UK).

2.3.3. Small-angle X-ray scattering (SAXS)

The structural characteristics of PoP and PoPQC samples varying in QC levels were investigated by SAXS analysis. SAXS measurements were performed on an Anton Paar SAXSpace camera in line collimation (0.5 × 20 mm beam size) with Cu-Kα radiation (λ = 1.54 Å) at room temperature (25 °C) with an exposure time of 1800s. The samples were filled into 1.5 mm quartz glass capillary tubes (QGCT 1.5) (Capillary Tube Supplies LTD, UK) and subsequently sealed to prevent evaporation. The investigations were carried out in a vacuum environment to minimise

the scattering caused by air. A 1D Mythen X-ray detector (Dectris Ltd., Baden, Switzerland) was used to record the scattering data. The 1D scattering curves were corrected for the primary beam position using SAXStreat (Anton Paar, Austria). The empty capillary and buffer solution profiles were used to subtract the background scattering. The background subtracted SAXS profiles were further analyzed by the indirect Fourier transformation approach (Bergmann & Glatter, 2000; Glatter, 1977) to obtain the real-space curves, i.e. the pair distance distribution function (PDDF) and the radius of gyration (R_g) could be calculated. The calibration has been done using the Silver Behenate and the exact sample to detector distance has been saved in the operating software of the SAXSPace instrument. The specific design for this setup enable controlling the sample to detector distance electronically with 0.001 mm precision.

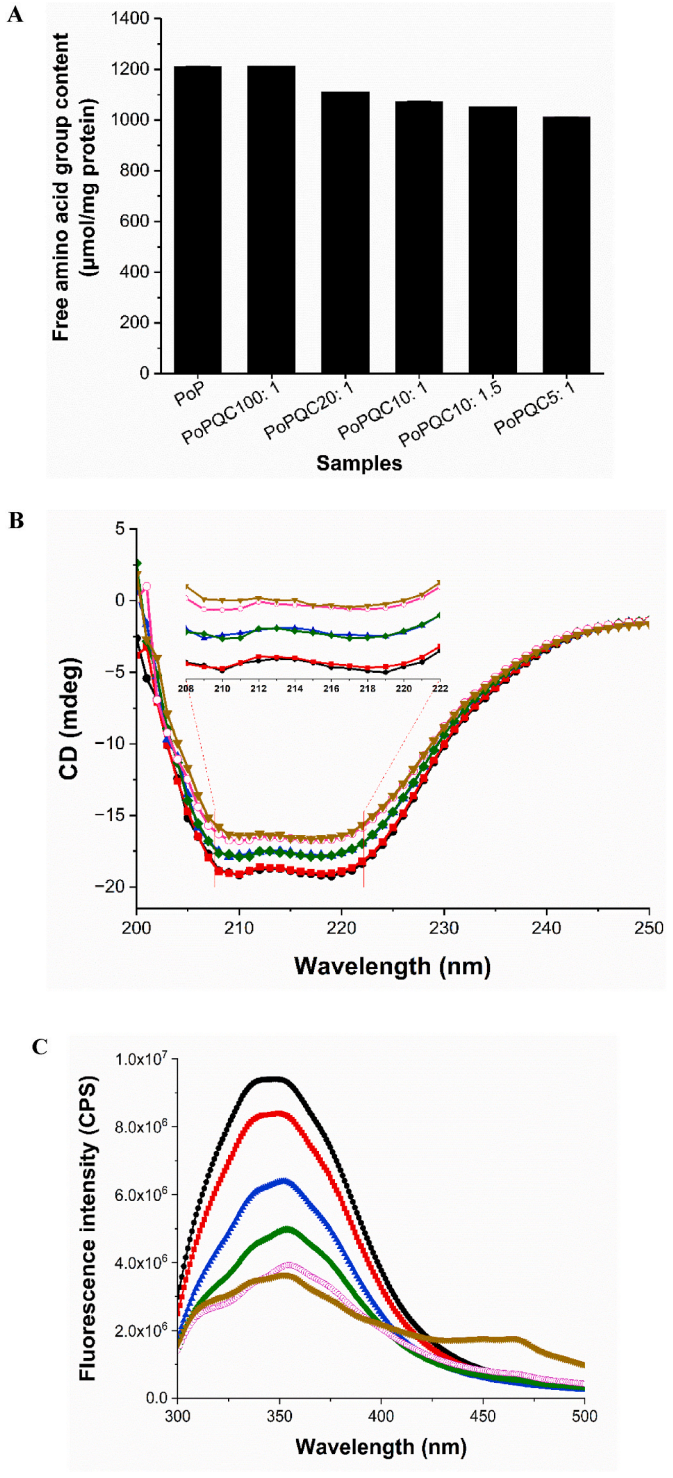

Fig. 1. Mean free amino acid contents (A), CD spectra (B), and fluorescence intensity (C) of PoP (●), PoPQC100: 1 (■), PoPQC20: 1 (▲), PoPQC10: 1 (♦), PoPQC10: 1.5 (○), and PoPQC5: 1 (▼) (n = 3 × 3). Excitation wavelength = 280 nm.

2.4. Conformational changes of hybrid PoPQC particles during conjugation

2.4.1. Free amino acid group determination

The free amino acid group contents and degree of conjugation (DC) of PoP and PoPQC were determined using a standardized *ortho*-phthaldialdehyde (OPA) method based on the study by Araiza-Calahorra, Akhtar, & Sarkar, 2020. Briefly, 3.81 g of sodium tetraborate, 0.088 g of dithiothreitol and 0.1 g sodium dodecyl sulphate (SDS) were mixed gently. The 0.08 g OPA was dissolved in 2 mL of methanol before Milli-Q water was added to make the final volume of OPA solution to 100 mL. The solution was kept in the dark before use. OPA solution (160 μL) was added to 1 mg/mL PoP or PoPQC in a disposable PMMA cuvette (45 × 12.5, H × W, 10 mm pathlength) and then mixed for 5 s; OPA mixed with HEPES buffer was used as a blank. The absorbance was measured at 340 nm using UV-VIS spectrophotometer (6715 UV/VIS Spectrophotometer, Jenway, UK). The degree of conjugation (DC) was be determined via the following equation:

$$Degree\ of\ conjugation\ (DC)\ \% = \frac{(C_{unconjugate} - C_{conjugate})}{C_{unconjugate}} \times 100\% \quad (1)$$

where, $C_{unconjugate}$ is the free amino acid content of PoP and $C_{conjugate}$ is the free amico acid content of the hybrid particles. A calibration curve of L-leucine solutions (0–200 μM) was used as a reference.

2.4.2. Circular dichroism (CD) analysis

A Chirascan Plus CD spectrophotometer was used. The PoP and PoPQC solutions were diluted with 20 mM HEPES buffer (pH 7.0) to obtain a protein concentration of 0.2 mg/mL. The diluted solution was injected into a 1 mm path length quartz sample cell at 20 °C. The scanning wavelength was selected to be between 200 and 250 nm with a bandwidth of 2 nm at a scan speed of 1 nm/s.

2.4.3. Fluorescence spectroscopy

PoP and PoPQC were diluted with Milli-Q water to 0.5 mg/mL (final protein concentration). The fluorescence emission spectra of PoP and PoPQC were recorded between 300 and 500 nm with the excitation wavelength fixed at 280 nm. The width of slit for both excitation and emission was set to 10 nm.

2.5. Preparation of Pickering emulsions (PEs)

PEs were prepared using commercially purchased sunflower oil (Tesco Supermarkets, UK) and PoPQC as a Pickering stabilizer at an oil: aqueous phase ratio of 1: 4 (v/v) with 1.0 wt% protein concentration in the final emulsions. Coarse emulsions were prepared by homogenization in an Ultra Turrax T25 homogenizer (IKA-Werke GmbH & Co., Staufen Germany) at 10,000 rpm for 1 min. The coarse emulsions were then passed twice through the Leeds Jet Homogenizer (two-chamber homogenizer, School of Food Science and Nutrition, University of Leeds, UK) at 300 bar to obtain fine emulsion droplets, abbreviated as E-PoPQC. A control, conventional emulsion was also prepared using PoP as emulsifier, abbreviated as E-PoP.

2.6. Droplet sizing

The emulsion droplet sizes were evaluated for a period of 6 months

Table 1
Degree of conjugation (DC) of hybrid particles with different amount of QC evaluated by OPA method.

Samples	Free amino acid group content (μmol/mg protein)	DC (%)
PoP	1213.14 ± 0.38[a]	control
PoPQC100: 1	1211.00 ± 1.03[a]	0.18 ± 0.08[e]
PoPQC20: 1	1110.81 ± 1.23[b]	8.44 ± 0.10[d]
PoPQC10: 1	1071.19 ± 7.46[c]	11.70 ± 0.62[c]
PoPQC10: 1.5	1051.33 ± 0.79[d]	13.34 ± 0.06[b]
PoPQC5: 1	1011.14 ± 0.71[e]	16.55 ± 0.06[a]

Mean values with different letters [(a-e)] within the same column are statistically different ($p < 0.05$).

using static light scattering using a Mastersizer (3000S series, Malvern Instruments Ltd, Malvern, UK). The average particle size was reported as the surface mean diameter ($d_{3,2}$) and the volume mean diameter ($d_{4,3}$), and the full particle size distribution (PSD).

2.6.1. Scanning electron microscopy (SEM)

The native PoP, QC, and hybrid PoPQC particles were mounted on specimen stubs then dried using hot air. The morphology of the samples was obtained using a Hitachi SU8230 FESEM (Hitachi, Japan). The images of all specimens were acquired at 2.0 mV, emission current was 21500 nA at a magnification of 50,000 × .

2.6.2. Cryogenic-scanning electron microscopy (cryo-SEM)

The microstructure of emulsions stabilized by PoP and hybrid PoPQC particles was characterized using a FEI – Helios G4 CX Dual beam FIB-SEM (Oregon, USA) with cryo-stage. Heptane was used instead of sunflower oil as the dispersed phase in order to mitigate the impact of oil crystallization during the freezing process (Araiza-Calahorra & Sarkar, 2019; Zhang et al., 2021c). The emulsion samples were positioned on sample stubs and flash-frozen in a liquid nitrogen at −180 °C prior to being transferred to the cryo-preparation chamber on the SEM. The frozen samples were subjected to −95 °C for 4 min then coated with 5 nm of platinum. Afterwards, the Pt-coated samples were transferred to the FEI chamber for imaging at −135 °C. The emulsion images were captured at 2.0 kV, 0.1 nA at magnifications of 100,000 ×.

2.6.3. Confocal scanning laser microscopy (CLSM)

The microstructure of the emulsions was also studied using a Zeiss LSM 880 inverted confocal microscope (Carl Zeiss MicroImaging GmbH, Jena, Germany). A stock solution of Nile Red (1 mg/mL) was used to stain the oil phase and a stock solution of Fast Green (1 mg/mL) was used to stain the protein phase. Nile Red and Fast Green were excited at wavelengths of 488 and 633 nm, respectively, while the auto-fluorescence of QC excitation was at 405 nm. To minimise the Brownian movement of oil droplets, the stained samples had been mixed with a sufficient amount of xanthan gum (1.0 wt %). Emulsion samples were placed into a laboratory-made welled slide and then gently covered by a coverslip (0.17 mm thickness) avoiding trapping air bubbles. A 63 × objective lens (oil immersion) was used to observe the emulsions.

2.7. Statistical analyses

Data are reported as means and standard deviations of at least three readings done on triplicate samples prepared on independent days. The statistical analyses were conducted using one-way ANOVA and multiple comparison test using SPSS software (IBM, SPSS statistics, version 24) and the significant difference between samples were considered when $p < 0.05$.

3. Results and discussion

3.1. Conjugation of PoP and QC to hybrid PoPQC particles

Firstly, we tested whether incorporation of QC affects the structural features of PoP during the fabrication of the hybrid PoPQC particles. Any changes in primary structure were tested for by measuring the free amino acid group content via the OPA method. The results are shown in Fig. 1A. At the lowest QC tested (PoP: QC100: 1) the free amino acid group content (~1210 μmol/mg protein) did not change significantly ($p \geq 0.05$). In fact, the free amino acid group content of PoPQC gradually reduced as the fraction of QC was increased beyond this level ($p < 0.05$). Phenolic hydroxyl groups in flavonoids such as QC may interact with proteins via hydrogen bonding through their –NH and –SH functional groups (Pan et al., 2023). The free amino acid group content was used to estimate the degree of conjugation (DC) of the hybrid particles, shown in Table 1. The DC ranged from 0.18% to 16.55% as the fraction of QC was increased. However, OPA reagent is composed of 1% SDS, which is a denaturant and may destroy non-covalent interactions between protein-protein or quercetin-protein, assuming that covalent interaction between PoP and QC may be responsible for decreasing in free amino acid group content (Cheng et al., 2020).

CD measurements in far-UV (200–250 nm) region were used to determine changes in protein secondary structure when conjugated with QC (Chen et al., 2018; Liu et al., 2017). The CD spectra of PoP and PoPQC are shown in Fig. 1B. The CD spectra of native PoP has a characteristic broad negative band containing two minima around 208 and 221 nm excited at 280 nm, indicating the existence of α–helix conformations (Cao & Xiong, 2015; Liu et al., 2017). The introduction of QC led to alterations in the CD spectra: the maximum negative ellipticities showed a gradual increase. This suggests unfolding of the PoP, decreasing in the α–helix content (Chen et al., 2018; Chen et al., 2020). The addition of QC to PoP may disrupt hydrogen bonding interactions between the carbonyl groups (C═O) and amino groups (–NH_2) in the α–helix structure (Cao & Xiong, 2015). This may lead to enhanced exposure of the PoP hydrophobic regions and strengthen its interaction with QC. The percentage of the secondary structures was calculated using BeStSel (Beta Structure Selection) and revealed that PoP composed of 77.8% α-helix, 15.5% β-sheet, and 6.7% unordered structure (Table S1.). After PoP complexed with QC, the content of α-helix decreased whilst the β-sheet slightly increased as a function of QC.

The intrinsic fluorescence spectra of proteins also offers insights into the molecular interactions associated with the conformational changes in their tertiary structure (Liu et al., 2017). The intrinsic fluorescence of PoP as a function of QC is shown in Fig. 1C. The fluorescence intensity of native PoP was maximal at ~349 nm, which may be attributed mainly to the intrinsic fluorescence of tryptophan (Trp) residues at this excitation wavelength (280 nm) (Chen et al., 2021; Du et al., 2022). There was a reduction in the maximum fluorescence intensity when QC was introduced, indicating a fluorescence quenching effect which may imply protein unfolding and a change in the polarity of the Trp microenvironment. Generally, Trp residues are located inside the hydrophobic core of the folded protein structure, which has a high quantum yield, resulting in a high fluorescence intensity. The fluorescence intensity reduces when the Trp residues are exposed to a hydrophilic environment due to the partially unfolded protein (Cao & Xiong, 2015; Cheng, Zhu, & Liu, 2020).

It was also noted that the wavelength of the maxium emission intensity of PoPQC shifted from 349 to 355 nm as the fraction of QC was increased. The presence of red-shift implies that the Trp residues of PoP were subjected to a hydrophilic environment, and fluorescence intensity decreases due to the interaction with QC, a quencher, providing additional evidence for the conformational changes of PoP. This suggests that the QC molecules become increasingly more embedded in the internal hydrophobic region core of the partial unfolded protein molecules, the aromatic rings of QC associating directly with Trp residues,

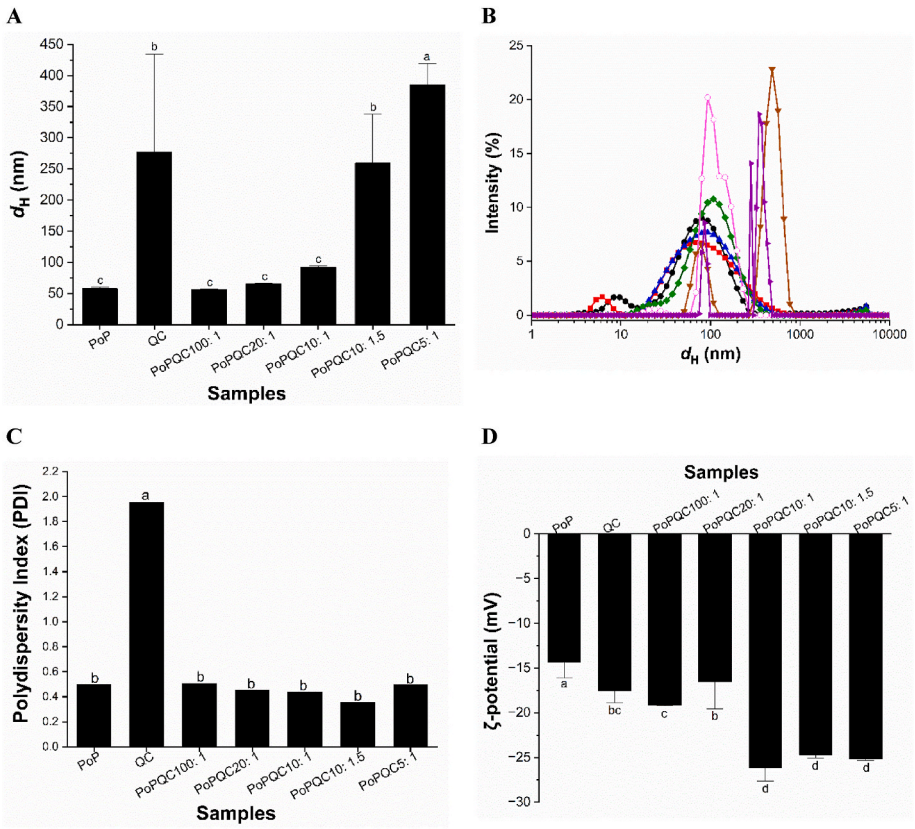

Fig. 2. Mean hydrodynamic diameter (d_H, black bars) (A), mean particle size distribution (B, black bars) of PoP (●), PoPQC100: 1 (■), PoPQC20: 1 (▲), PoPQC10: 1 (◆), PoPQC10: 1.5 (○), and PoPQC5: 1 (▼) and QC (▶), mean PDI (C, black bars), and mean ζ-potential (black bars) (D). Error bars represent standard deviation (n = 3 × 3). Parameters denoted with the same lower case subscripts do not differ statistically at the confidence of $p \geq 0.05$.

which have been shown to act as specific binding sites for other hydrophobic bioactive compounds (Chen et al., 2021; Cuevas-Bernardino et al., 2018; Du et al., 2022; Fang et al., 2011). The fluorescence quenching mechanism of QC with PoP was calculated from the maximum fluorescence intensity of PoP according to Stern-Volmer equation:

$$\frac{F_0}{F} = 1 + K_{sv}[Q] \quad (2)$$

where, F_0 and F are the maximum fluorescence intensity of PoP without quencher and hybrid particles with different concentrations of QC, respectively. [Q] is QC concentration (mM), and K_{SV} is the Stern-Volmer quenching constant.

The fitted Stern-Volmer plot of PoP and QC fluorescence quenched by varying concentrations of QC exhibited a linear relationship of quenching interaction between PoP and QC. The K_{sv} values of PoP and hybrid particles are shown in Table S2, which indicates a binding between PoP and QC. The K_{sv} values decreased as a function of QC concentration suggesting that QC possessed the capability to quench the intrinsic fluorescence of the hybrid particles (Gong et al., 2021; Li et al., 2023). In summary, the addition of QC resulted in partially unfolded PoP under natural conditions, and the major interactions between QC and PoP were predominantly attributed to hydrogen bonding and hydrophobic interactions.

3.2. Physicochemical and nanostructural characteristics of hybrid PoPQC particles

The mean particle sizes, PSDs, polydispersity (PDI) and ζ-potential of native PoP and PoPQC are presented in Fig. 2. The hydrodynamic diameter (d_H) of PoP and QC were measured as 57 and 277 nm, respectively. Of more importance than these exact values, the addition of QC is seen to cause a significant increase in d_H of the hybrid particles to 385 nm ($p < 0.05$), although there was no significant difference when the mass ratio of hybrid particles was between PoPQC100: 1 and PoPQC10: 1 (Fig. 2A). Particularly, with the highest PoPQC ratio the d_H was higher than QC alone (277 nm), which suggests protein-induced aggregation of the QC (Han et al., 2022). The PSDs of the native PoP and hybrid particles determined by DLS are illustrated in Fig. 2B. The PoP showed two main peaks between 7 and 300 nm, in agreement with Kew et al. (2021), representing the protein monomer and its aggregates, respectively. Meanwhile, QC showed a polymodal distribution between 86 nm and 364 nm and the highest PDI (1.953) among the samples tested ($p < 0.05$). The hybrid PoPQC particles, particularly with the low QC, showed a single the main peak in the 100 nm range with low PDI (Fig. 2C). It is to be expected that QC should have the largest PDI ($p < 0.05$) since it is largely insoluble in water and its crystals are anisotropic (rod-shaped) (Zembyla, Murray, & Sarkar, 2018) whilst the dynamic light scattering (DLS) fits all the distribution to spherical form factor. The mean d_H of QC should therefore be taken with caution.

Both PoP and QC apparently had negative charge at pH 7.0, with ζ-potentials of −14.4 and −19.2 mV, respectively. The negative charge of PoP is attributed to the abundance of anionic groups (Hussain et al., 2021b; Li, 2023), whilst the dissociation of the C_7–OH on the QC nucleus proceeds in alkaline conditions which could account for the presence of the negative charge (Zembyla et al., 2018). Interestingly, hybrid particles exhibited a significant increase in the magnitude of the negative values of their ζ-potential relative to PoP and QC alone (Fig. 2D) (the exception being the ratio PoPQC20: 1). This is not straightforward to interpret from this type of measurement, but again hints at significant rearrangement of the structure of the PoP and the binding of the QC.

In order to probe the structure deeper in length scales, PoP and

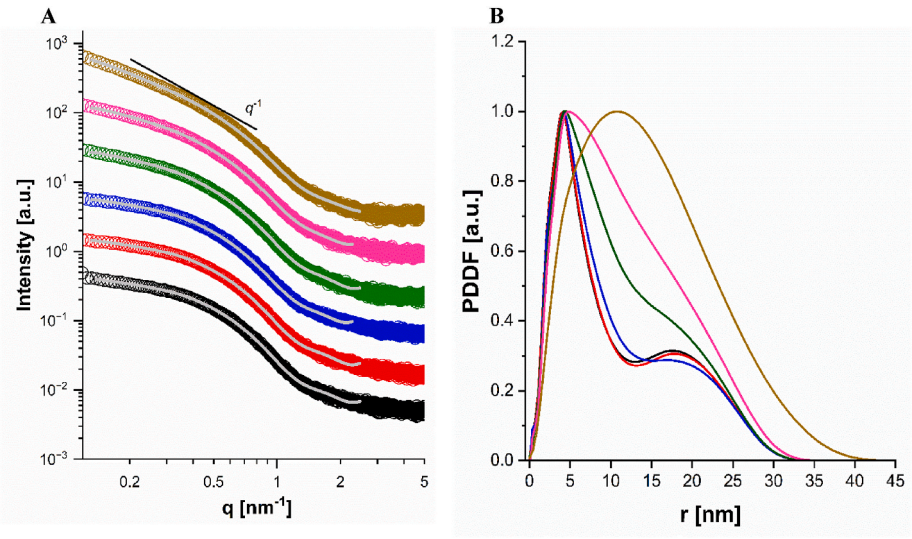

Fig. 3. SAXS profiles (A) and radius of gyration (R_g) (B) of PoP (○, —), PoPQC100: 1 (○, —), PoPQC20: 1 (○, —), PoPQC10: 1 (○, —), PoPQC10: 1.5 (○, —), and PoPQC5: 1 (○, —).

hybrid PoPQC particles were also analyzed by SAXS (Fig. 3). The significant increase in scattering intensity in the low q region as well as the shifts in the form of the scattering profile of hybrid particles in relation to the variation in QC is apparent. All SAXS curves intensities decreased slightly at small q ($q < 0.5$), whilst decreased sharply at the large $q > 0.5$. The decay of scattering intensity is significantly faster at small q values, particularly in the case of complexation with a large proprtions of QC (PoPQC20: 1 to PoPQC5: 1) (Fig. 3A), indicating that the large hybrid particles are being formed (Cheng et al., 2022). The changes in the slope of intensity of PoP and PoPQC demonstrated the changes in the structural characteristics of the hybrid PoPQC particles (Boukari, Lin, & Harris, 1997; Cheng et al., 2019). The pair-distance distribution function (PDDF) of native PoP and the hybrid PoPQC particles are shown in Fig. 3B. The PDDF of native PoP demonstrated a maximum dimension of 32 nm and a radius of gyration (R_g) of 9.35 nm in solution, being comparable with the crystalline dimensions of PoP, well characterized previously (Green et al., 2013; Rydel et al., 2003). The PDDF also shows a bimodal pair-distance distribution, which most likely originate from the small and the large molecular weight proteins of PoP (*i.e.* patatin and the potato multicystatin).

Patatin is the predominant protein with a molecular weight ranging from 40 to 42 kDa glycoproteins. Potato multicystatin is a protease inhibitor which presents in high quantities as distinct crystals in the cortical parenchyma cells, molecular weight of these crystals ranges from 5 to 25 μm (Schmidt, Damgaard, Greve-Poulsen, Larsen, & Hammershøj, 2018; Schmidt et al., 2019; Waglay et al., 2014). However, it may also be plausible that some sort of complexation occurs between patatin and the protease inhibitory proteins available in PoP, leading to a dumbbell like structure formation, showing a bimodal PPDF. The SAXS analysis reveals minimal changes in the PoP nanoscale structure upon addition of low content of QC (PoPQC100: 1 and PoPQC20: 1). In the presence of high QC content, the SAXS profiles show a faster decay at small q values (following an intensity decay by q^{-1}) and the PDDF represents an asymmetric size distribution with a right-truncated shape that almost linearly decays in the right tail and stretches up to 42 nm in the case of PoPQC5: 1. Such asymmetric behaviour in pair-distance distribution function is an indication of elongated structures, likely originating from the elongated proteins and/or complexation and aggregation of PoP facilitated by hydrophobic region of QC (Glatter, 2018; Liu et al., 2021), in line with the structural changes observed in Fig. 1.

The morphology of PoP, QC and PoPQC was also observed via SEM, as shown in Fig. 4. The native PoP appeared as relatively small and spherical particles (Fig. 4A), in agreement with the findings of Hussain et al., 2021b, whilst QC exhibited the classic, rod-like crystalline shape (Fig. 4B) (Zembyla, Murray, Radford, & Sarkar, 2019). As the PoPQC mass ratio increased, the morphology of the PoPQC ranged from bridged individual, spherical-type particles to a more condensed and larger network-like structure of such particles (Fig. 4C–E). The surfaces of the aggregated PoPQC particles at low QC contents appeared to be smooth (Fig. 4C–E), but as the proportion of QC increased the particles started to appear more polyhedral (Fig. 4F and G) with rough edges. This is possibly QC crystals starting to be revealed, embedded within the mixed structure. As always, however, it is possible that some of these structures might be influenced to some extent by the SEM sample preparation.

3.3. *Emulsion and Pickering emulsion stabilization by PoP, hybrid POPQC particles, and storage stability*

Having characterized the properties of hybrid particles on their own, their behaviour as Pickering emulsion (PE) stabilizers was assessed. Cryo-SEM images of PEs stabilized by PoPQC are shown in Fig. 5A–F with zoomed in regions focusing on the oil-water interface. The microstructure of the interfacial layer most notably varied as the QC contents of the PoPQC particles was varied. At low QC contents (Fig. 5B) the interfaces appeared to be covered by small and smooth spherical structures. With hybrid PoPQC particles of higher QC content, densely interconnected stuctures were seen at the interface (Fig. 5C–F), similar to the structures observed for the hybrid particles on their own (Fig. 4).

Emulsion stability was also observed over 6 months storage at 4 °C, via particle sizing, ζ-potential and confocal microscopy (CLSM) and macroscopic images are presented in Fig. S1. The droplet characteristics were measured at neutral pH (7.0) and room temperature (25 °C), shown in Table 2. The PSDs are shown in Fig. 6. At the beginning of the storage time $d_{4,3}$ of E-PoP was smallest with a monomodal droplet size distribution. The mean diameter of the fresh emulsions increased (e.g., $d_{4,3}$ from 1.4 to 43.4 μm) significantly ($p < 0.05$) with increasing QC content of the PoPQC (Table 2) although all the PSDs were monomodal (Fig. 6A) except for E-PoPQC10: 1.5 and E-PoPQC5: 1 (Fig. 6B–F). Large

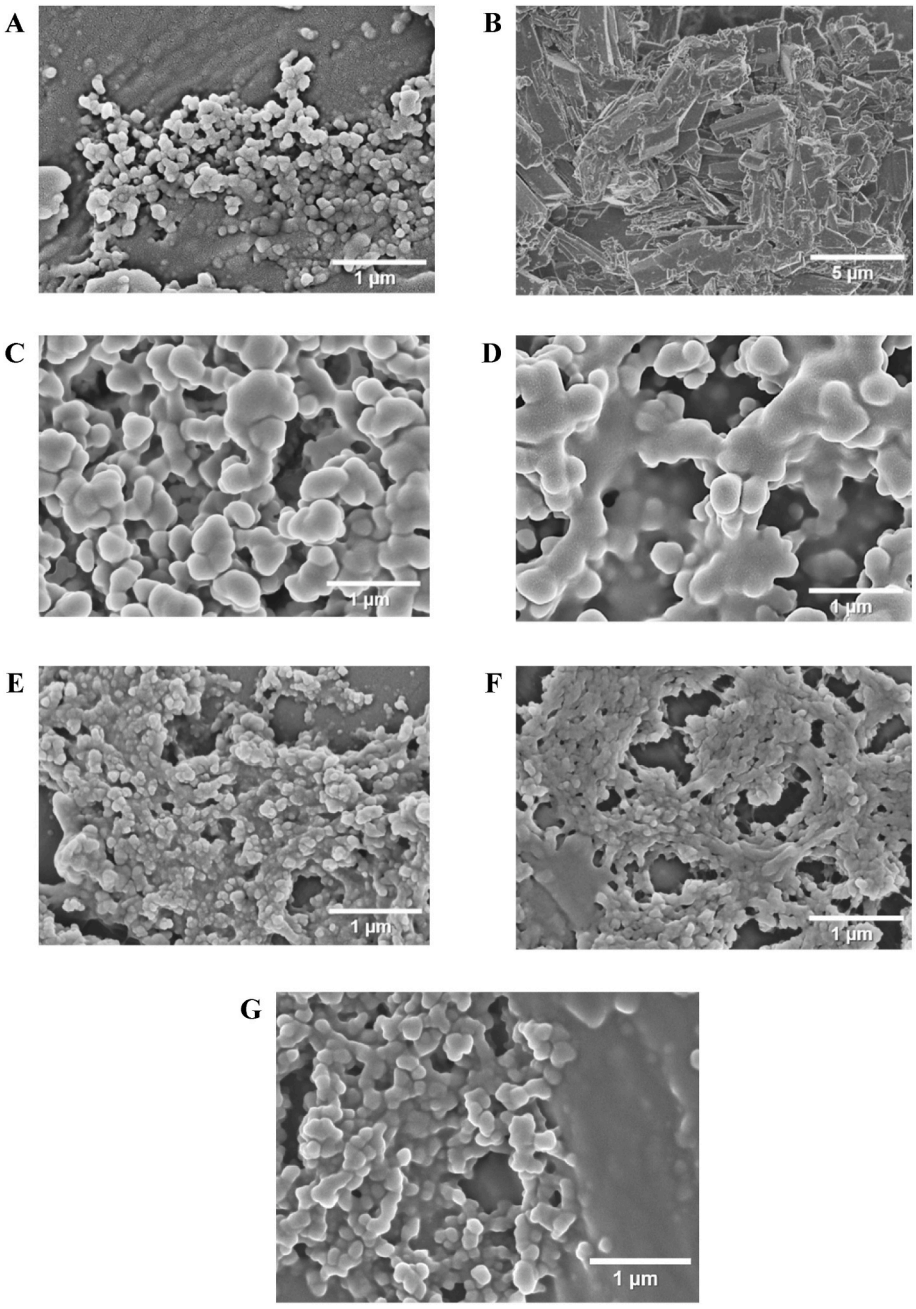

Fig. 4. The SEM micrographs of PoP (A), QC (B), PoPQC100: 1(C), PoPQC20: 1 (D), PoPQC10: 1.0 (E), PoPQC10: 1.5 (F), and PoPQC5: 1 (G). Scale bar is 1 μm.

droplet sizes are expected when the stabilizing particles are larger. The ζ-potential of the freshly emulsions ranged from −16 to −27 mV (Table 2).

Over 6-months storage, $d_{3,2}$ and $d_{4,3}$ of E-PoP increased, the PSD became wider and bimodal (Fig. 6A–Table 2) indicating coalescence. On the contrary, $d_{3,2}$ and $d_{4,3}$ for E-PoPQC100: 1 and E-PoPQC 20: 1 exhibited minimal variation over the storage period (Fig. 6B and C). The remaining E-PoPQCs, i.e., with higher QC contents, showed *decreases* in droplet size whilst remaining polymodal (Fig. 6D–F). This apparent reduction must have been due to the rapid rise of flocs of droplets towards the top of the samples, hindering their detection for droplet size analysis. The ζ-potential of all emulsion samples showed only a slight change over 6-months storage (Table 2).

The microstructure of the fresh and 6-months old PEs was evaluated using confocal microscopy (CLSM), shown in Fig. 7. The CLSM micrographs indicated that all emulsion samples showed the formation the interfacial layers of either PoP or PoPQC (labelled green for PoP, and labelled yellow for QC) (Fig. 7A1-7F1). The aqueous phase of the emulsions shows a green colour indicating the presence of unadsorbed protein. The images confirmed the larger droplet sizes of the PoPQC-stabilized emulsions compared to E-PoP (Fig. 7A1-7A2). More importantly, all the PEs (Fig. 7B1–7F1, 7B2–7F2) showed bridging of droplets due to the formation of a connected network in the continuous phase, potentially inhibiting coalescence. These networks resembled those formed by the particles on their own (Fig. 4). Consequently, any emulsion stabilizing effects of the PoPQC particles could be due to both their adsorption and/or this network formation in the bulk. This needs further characterization in the future.

4. Conclusions

Hybrid particles of PoP and QC have been successfully fabricated

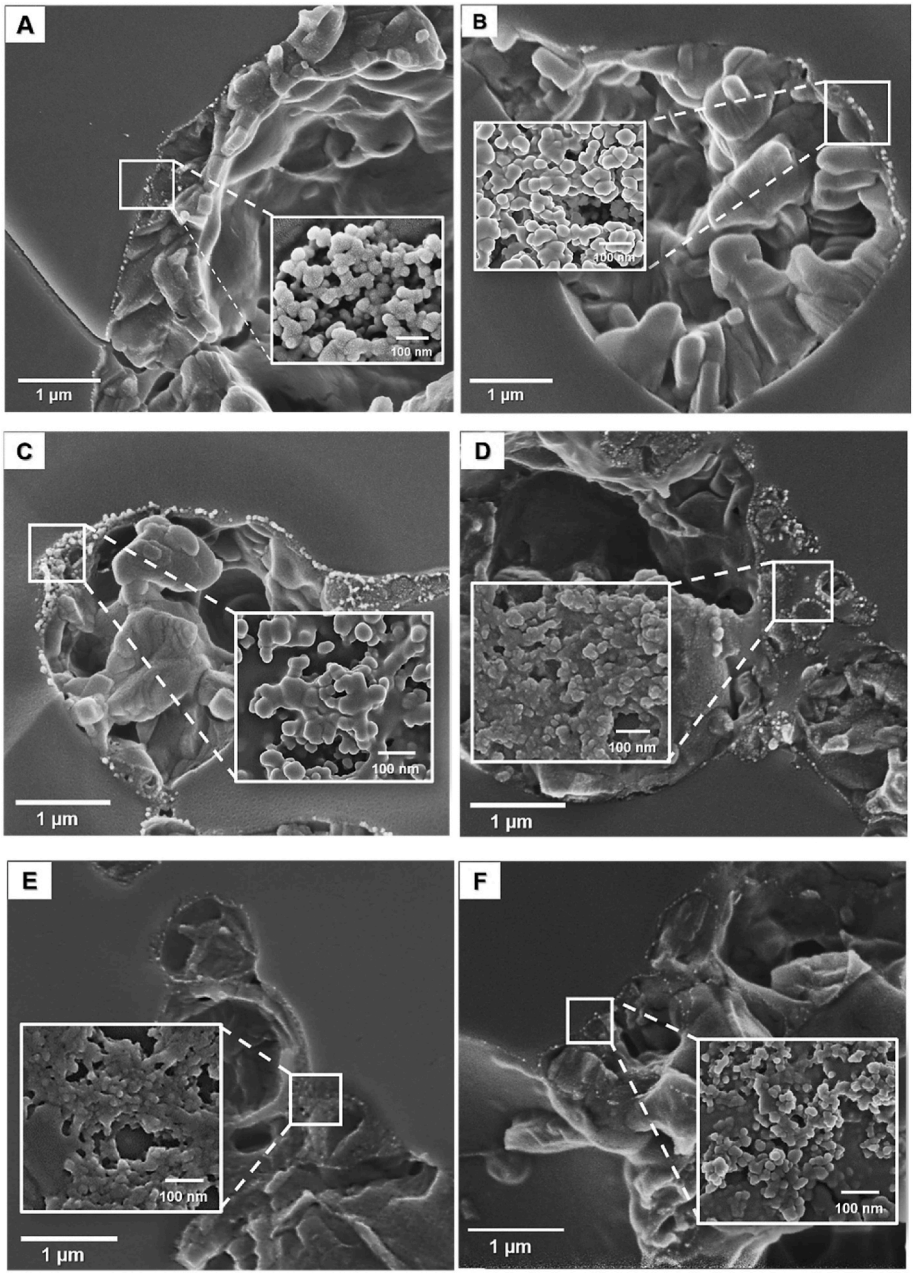

Fig. 5. Cryo-SEM of emulsions stabilized by PoP (A), and Pickering emulsions stabilized by PoPQC100: 1(B), PoPQC20: 1 (C), PoPQC10: 1.0 (D), PoPQC10: 1.5 (E), and PoPQC5: 1 (F), respectively. The smaller inserts are zoomed in regions of the interface. The scale bars are 1 μm in the larger micrographs and 100 nm in the zoomed in regions, respectively.

under ambient conditions and used to stabilize Pickering oil-in-water (O/W) emulsions over 6 months storage. The PoP and QC were complexed spontaneously via non-covalent interactions, particularly hydrophobic interactions, and hydrogen bonding causing conformational changes in the protein structure. The obtained hybrid PoPQC particles were spherical but tended to aggregate and interconnect in the bulk as their QC content was increased. Indeed, this increased aggregation also appeared to occur at the interface of the emulsion droplets and also in the bulk aqueous phase of the emulsions. This aggregation contributed to greater stability to coalescence of the PoPQC-stabilized emulsions compared to the conventional emulsions stabilized by PoP alone, although the mean droplet sizes of the latter were still smaller. These findings should provide impetus to fabricating novel food-grade hybrid particle stabilizers with dual functionality but based on more sustainable, plant-based ingredients and simple, physical processing. Ongoing studies are focusing on interfacial properties and structure of the adsorbed films of hybrid PoPQC particles to pinpoint more clearly the effects of PoP vs QC on the physicochemical and biophysical implications for the corresponding emulsions.

CRediT authorship contribution statement

Nisufyan Nimaming: Writing – original draft, Methodology, Investigation, Data curation, Conceptualization. **Amin Sadeghpour:** Writing – review & editing, Supervision, Investigation, Conceptualization. **Brent S. Murray:** Writing – review & editing, Supervision, Investigation, Conceptualization. **Anwesha Sarkar:** Writing – review & editing, Supervision, Investigation, Conceptualization.

Table 2
Evolution of mean droplet size ($d_{3,2}$, $d_{4,3}$) and ζ-potential of conventional emulsions stabilized by PoP and Pickering emulsions stabilized by hybrid PoPQC particles over 6 months of storage.

Samples	Droplet size (μm)						ζ-potential (mV)		
	$d_{3,2}$			$d_{4,3}$					
	fresh	1 month	6 months	fresh	1 month	6 months	fresh	1 month	6 months
E-PoP	0.3 ± 0.01^{eB}	0.2 ± 0.01^{fC}	0.9 ± 0.03^{bA}	1.4 ± 0.02^{eB}	1.1 ± 0.11^{dC}	4.9 ± 1.19^{bA}	-16.6 ± 1.50^{aA}	-33.6 ± 0.25^{dC}	-29.0 ± 0.36^{cB}
E-PoPQC100: 1	1.3 ± 0.01^{dA}	0.8 ± 0.01^{eB}	0.6 ± 0.17^{cB}	2.8 ± 0.03^{dA}	1.7 ± 0.04^{cdB}	2.5 ± 0.24^{bcA}	-26.2 ± 0.95^{bcA}	-28.2 ± 0.22^{bB}	-30.3 ± 1.35^{cC}
E-PoPQC20: 1	1.5 ± 0.01^{cA}	0.9 ± 0.02^{dB}	0.3 ± 0.11^{dC}	2.8 ± 0.03^{dA}	2.5 ± 0.11^{cB}	1.8 ± 0.13^{cC}	-26.5 ± 1.00^{bcA}	-32.5 ± 0.41^{dC}	-28.3 ± 0.31^{bcB}
E-PoPQC10: 1	4.4 ± 0.04^{aA}	1.9 ± 0.02^{cB}	0.2 ± 0.01^{eC}	5.8 ± 0.08^{cA}	2.3 ± 0.06^{cB}	1.3 ± 0.03^{dC}	-27.0 ± 1.18^{cA}	-29.4 ± 0.06^{bcB}	-32.1 ± 0.65^{dC}
E-PoPQC10: 1.5	3.3 ± 0.02^{bA}	3.1 ± 0.02^{bB}	0.3 ± 0.06^{dC}	15.9 ± 0.83^{bA}	7.7 ± 0.11^{bB}	2.7 ± 0.13^{bcC}	-27.3 ± 0.40^{cA}	-31.0 ± 1.77^{bcB}	-27.0 ± 1.02^{bA}
E-PoPQC20: 1	4.4 ± 0.02^{aB}	4.8 ± 0.13^{aA}	3.3 ± 0.13^{aC}	43.4 ± 0.50^{aA}	34.7 ± 1.30^{aB}	11.8 ± 1.85^{aC}	-24.4 ± 1.32^{bC}	-22.6 ± 5.17^{aB}	-20.9 ± 4.17^{aA}

Mean values with different lowercase letters [a-f] with the same column, and uppercase letters [A–C] with the same row indicate significant differences ($p < 0.05$).

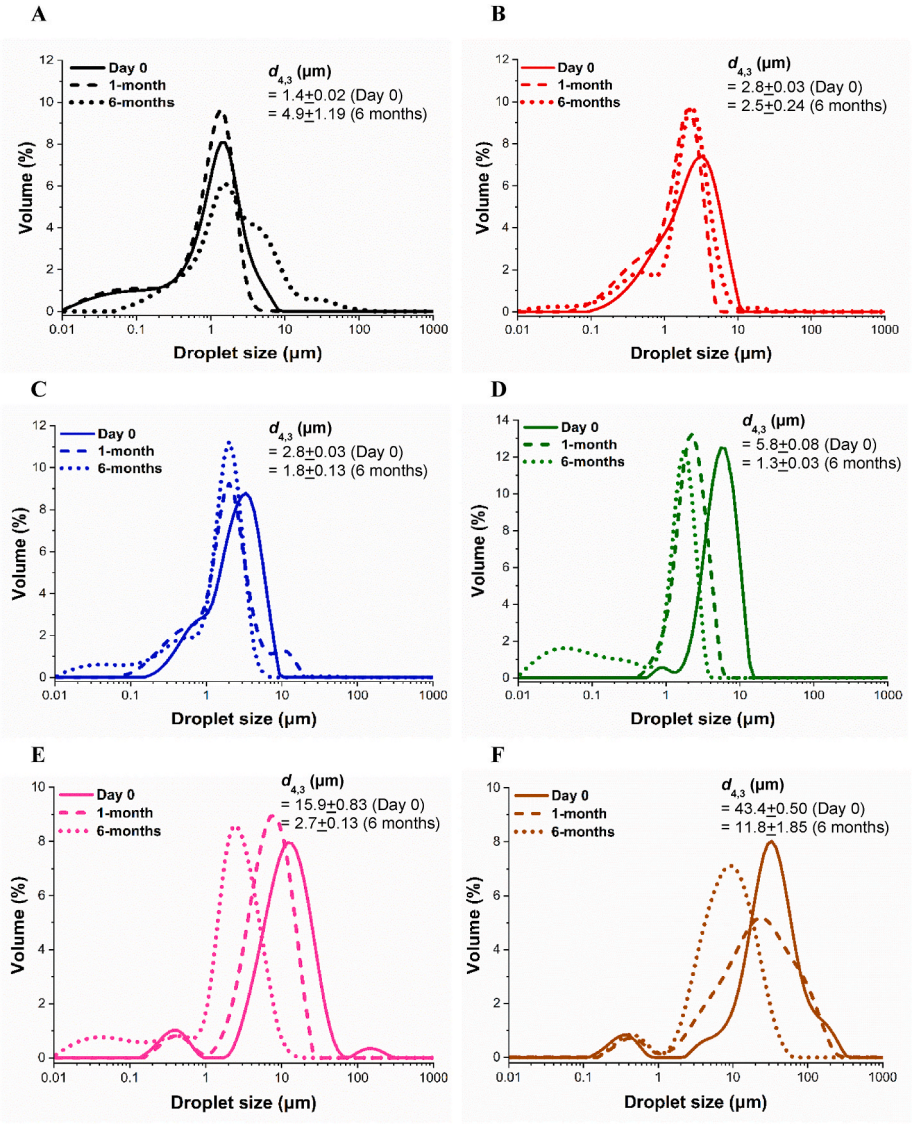

Fig. 6. Mean droplet size distribution of emulsions stabilized by PoP (A) PoPQC100: 1 (B), PoPQC20: 1 (C), PoPQC10: 1 (D), PoPQC10: 1.5 (E), and PoPQC5: 1 (F) over 6 months of storage at 4 °C (n = 2 × 3).

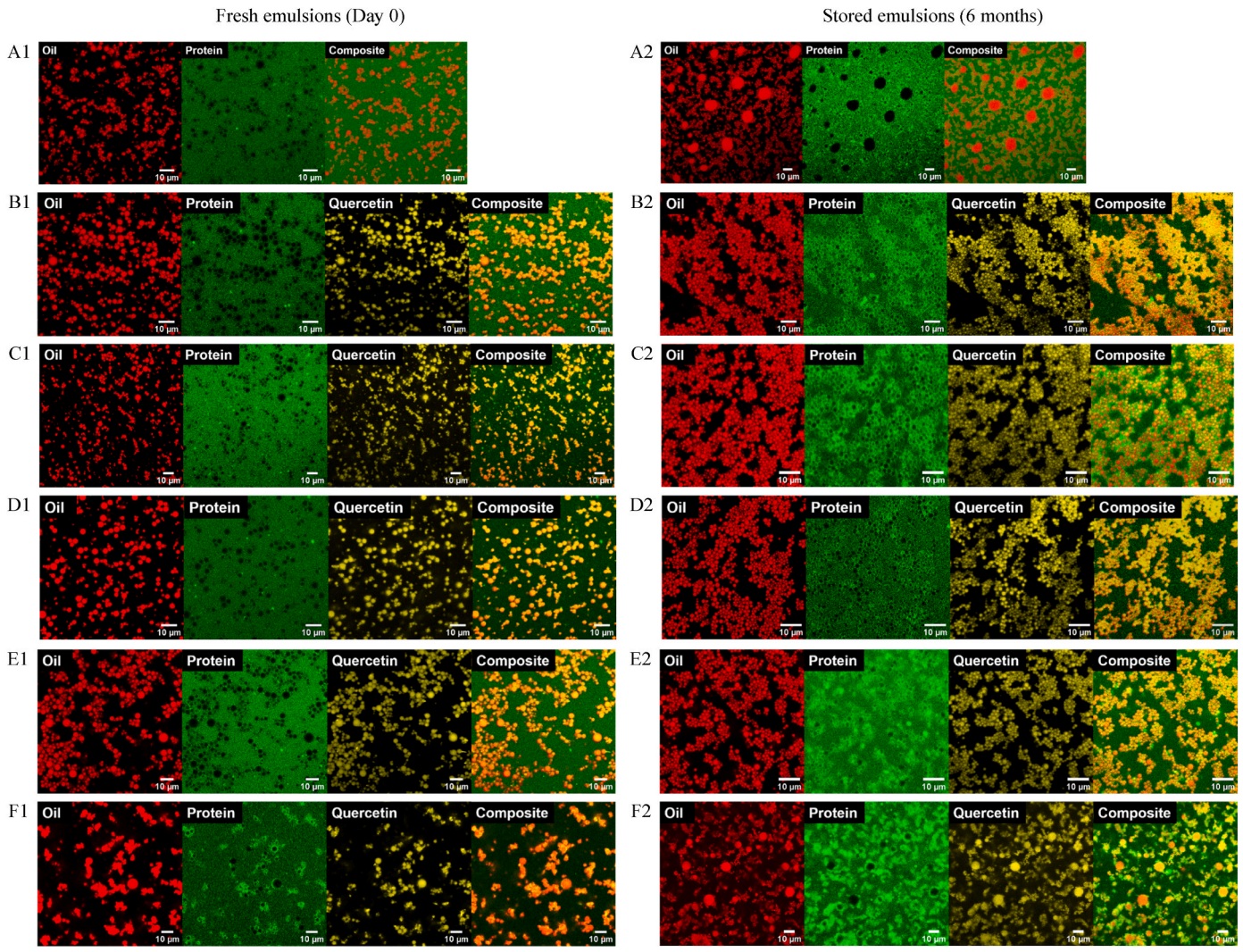

Fig. 7. Confocal microscopy images of fresh and 6 months-stored emulsion stabilized by PoP (A1, A2), PoPQC100: 1 (B1, B2), PoPQC20: 1 (C1, C2), PoPQC10: 1 (D1, D2), PoPQC10: 1.5 (E1, E2), and PoPQC5: 1 (F1, F2). The red and green colour represent the oil (stained by Nile Red) and protein phase (stained by Fast Green), respectively; whilst QC is autofluorescent with excitation of 405 nm and composite was a merge of all three channels (oil, protein and quercetin).

Declaration of competing interest

The authors declare that they have no known competing financial interests or personal relationships that could have appeared to influence the work reported in this paper.

Data availability

Data will be made available on request.

Acknowledgements

Author NN acknowledges research financial support from the Rajamangala University of Technology Krungthep (RMUTK), Thailand, for a PhD academic scholarship. Authors thank Mr. G Nasir Khan, Dr. Ruth Hughes from Faculty of Biological Sciences, and Mr. Stuart Micklethwaite from Faculty of Engineering and Physical Sciences at University of Leeds for their technical support for CD analysis, CLSM and cryo-SEM imaging.

Appendix A. Supplementary data

Supplementary data to this article can be found online at https://doi.org/10.1016/j.foodhyd.2024.110146.

References

Aery, S., Parry, A., Araiza-Calahorra, A., Evans, S. D., Gleeson, H. F., Dan, A., & Sarkar, A. (2023). Ultra-stable liquid crystal droplets coated by sustainable plant-based materials for optical sensing of chemical and biological analytes [10.1039/D3TC00598D]. *Journal of Materials Chemistry C, 11*(17), 5831–5845. https://doi.org/10.1039/D3TC00598D

Araiza-Calahorra, A., Akhtar, M., & Sarkar. (2020). Conjugate microgel-stabilized Pickering emulsions: Role in delaying gastric digestion. *Food Hydrocolloids, 105*, 105794. https://doi.org/10.1016/j.foodhyd.2020.105794

Araiza-Calahorra, A., & Sarkar, A. (2019). Pickering emulsion stabilized by protein nanogel particles for delivery of curcumin: Effects of pH and ionic strength on curcumin retention. *Food Structure, 21*, 100113. https://doi.org/10.1016/j.foostr.2019.100113

Bergmann, A., & Glatter, G. F. O. (2000). Solving the generalized indirect Fourier transformation (GIFT) by Boltzmann simplex simulated annealing (BSSA). *Journal of Applied Crystallography, 33*(5), 1212–1216. https://doi.org/10.1107/S0021889800008372

Binks, B. P. (2002). Particles as surfactants—similarities and differences. *Current Opinion in Colloid & Interface Science, 7*(1), 21–41. https://doi.org/10.1016/S1359-0294(02)00008-0

Boukari, H., Lin, J. S., & Harris, M. T. (1997). Small-angle X-ray scattering study of the formation of colloidal Silica particles from Alkoxides: Primary particles or not? *Journal of Colloid and Interface Science, 194*(2), 311–318. https://doi.org/10.1006/jcis.1997.5112

Cao, Y., & Xiong, Y. L. (2015). Chlorogenic acid-mediated gel formation of oxidatively stressed myofibrillar protein. *Food Chemistry, 180*, 235–243. https://doi.org/10.1016/j.foodchem.2015.02.036

Carpentier, J., Conforto, C., Chaigneau, C., Vendeville, J.-E., & Maugard, T. (2022). Microencapsulation and controlled release of α-tocopherol by complex coacervation between pea protein and tragacanth gum: A comparative study with Arabic and tara gums. *Innovative Food Science & Emerging Technologies, 77*, Article 102951. https://doi.org/10.1016/j.ifset.2022.102951

Chen, N., Lin, L., Sun, W., & Zhao, M. (2014). Stable and pH-sensitive protein nanogels made by self-assembly of heat denatured soy protein. *Journal of Agricultural and Food Chemistry, 62*(39), 9553–9561. https://doi.org/10.1021/jf502572d

Chen, Y., Hu, J., Yi, X., Ding, B., Sun, W., Yan, F., Wei, S., & Li, Z. (2018). Interactions and emulsifying properties of ovalbumin with tannic acid. *LWT, 95*, 282–288. https://doi.org/10.1016/j.lwt.2018.04.088

Chen, Y., Li, Z., Yi, X., Kuang, H., Ding, B., Sun, W., & Luo, Y. (2020). Influence of carboxymethylcellulose on the interaction between ovalbumin and tannic acid via noncovalent bonds and its effects on emulsifying properties. *LWT, 118*, Article 108778. https://doi.org/10.1016/j.lwt.2019.108778

Chen, Y., Yao, M., Peng, S., Fang, Y., Wan, L., Shang, W., … Zhang, W. (2023). Development of protein-polyphenol particles to stabilize high internal phase Pickering emulsions by polyphenols' structure. *Food Chemistry, 428*, 136773. https://doi.org/10.1016/j.foodchem.2023.136773

Chang, C., Li, J., Su, Y., Gu, L., Yang, Y., & Zhai, J. (2022). Protein particle-based vehicles for encapsulation and delivery of nutrients: Fabrication, digestion, and release properties. *Food Hydrocolloids, 123*. https://doi.org/10.1016/j.foodhyd.2021.106963

Chen, C., Shi, K., Qin, X., Zhang, H., Chen, H., Hayes, D. G., Wu, Q., Hu, Z., & Liu, G. (2021). Effect of interactions between glycosylated protein and tannic acid on the physicochemical stability of Pickering emulsions. *LWT, 152*, Article 112383. https://doi.org/10.1016/j.lwt.2021.112383

Cheng, J., Zhu, M., & Liu, X. (2020). Insight into the conformational and functional properties of myofibrillar protein modified by mulberry polyphenols. *Food Chemistry, 308*, 125592. https://doi.org/10.1016/j.foodchem.2019.125592

Cheng, L., Ye, A., Hemar, Y., Gilbert, E. P., de Campo, L., Whitten, A. E., & Singh, H. (2019). Interfacial structures of droplet-stabilized emulsions formed with whey protein microgel particles as revealed by small- and ultra-small-angle neutron scattering. *Langmuir, 35*(37), 12017–12027. https://doi.org/10.1021/acs.langmuir.9b01966

Cheng, L., Ye, A., Yang, Z., Gilbert, E. P., Knott, R., de Campo, L., … Singh, H. (2022). Small-angle X-ray scattering (SAXS) and small-angle neutron scattering (SANS) study on the structure of sodium caseinate in dispersions and at the oil-water interface: Effect of calcium ions. *Food Structure, 32*, 100276. https://doi.org/10.1016/j.foostr.2022.100276

Zhou, F. -Z., Yan, L., Yin, S. -W., Tang, C. -H., & Yang, X. -Q. (2018). Development of pickering emulsions stabilized by gliadin/proanthocyanidins hybrid particles (GPHPs) and the fate of lipid oxidation and digestion. *Journal of Agricultural and Food Chemistry, 66*(6), 1461–1471. https://doi.org/10.1021/acs.jafc.7b05261

Cuevas-Bernardino, J. C., Leyva-Gutierrez, F. M. A., Vernon-Carter, E. J., Lobato-Calleros, C., Román-Guerrero, A., & Davidov-Pardo, G. (2018). Formation of biopolymer complexes composed of pea protein and mesquite gum – impact of quercetin addition on their physical and chemical stability. *Food Hydrocolloids, 77*, 736–745. https://doi.org/10.1016/j.foodhyd.2017.11.015

Dai, T., Li, T., Li, R., Zhou, H., Liu, C., Chen, J., & McClements, D. J. (2020). Utilization of plant-based protein-polyphenol complexes to form and stabilize emulsions: Pea proteins and grape seed proanthocyanidins. *Food Chemistry, 329*, 127219. https://doi.org/10.1016/j.foodchem.2020.127219

David, S., & Livney, Y. D. (2016). Potato protein based nanovehicles for health promoting hydrophobic bioactives in clear beverages. *Food Hydrocolloids, 57*, 229–235. https://doi.org/10.1016/j.foodhyd.2016.01.027

Dickinson, E. (2012). Use of nanoparticles and microparticles in the formation and stabilization of food emulsions. *Trends in Food Science & Technology, 24*(1), 4–12. https://doi.org/10.1016/j.tifs.2011.09.006

Du, C. -X., Xu, J., Luo, S. -Z.., Li, X. J. -J., Mu, J., Mu, D. -D., … Zheng, Z. (2022). Low-oil-phase emulsion gel with antioxidant properties prepared by soybean protein isolate and curcumin composite nanoparticles. *LWT, 161*, 113346. https://doi.org/10.1016/j.lwt.2022.113346

Edelman, R., Engelberg, S., Fahoum, L., Meyron-Holtz, E. G., & Livney, Y. D. (2019). Potato protein- based carriers for enhancing bioavailability of astaxanthin. *Food Hydrocolloids, 96*, 72–80. https://doi.org/10.1016/j.foodhyd.2019.04.058

Fang, R., JIng, H., Chai, Z., Zhao, G., Stoll, S., Ren, F., … Leng, X. (2011). Design and characterization of protein-quercetin bioactive nanoparticles. *J Nanobiotechnology, 9*, 19. https://doi.org/10.1186/1477-3155-9-19

Fu, D., Deng, S., McClements, D. J.., Zou, L., Zou, L., Yi, J., … Liu, W. (2019). Encapsulation of β-carotene in wheat gluten nanoparticle-xanthan gum-stabilized Pickering emulsions: Enhancement of carotenoid stability and bioaccessibility. *Food Hydrocolloids, 89*, 80–89. https://doi.org/10.1016/j.foodhyd.2018.10.032

Glatter, O. (1977). A new method for the evaluation of small-angle scattering data. *Journal of Applied Crystallography, 10*(5), 415–421. https://doi.org/10.1107/S0021889877013879

Glatter, O. (2018). *Scattering methods and their application in colloid and interface science*. https://doi.org/10.1107/S1600576718016023

Gong, S., Yang, C., Zhang, J., Ying, Y., Gu, X., Li, W., & Wang, Z. (2021). Study on the interaction mechanism of purple potato anthocyanins with casein and whey protein. *Food Hydrocolloids, 111*, 106223. https://doi.org/10.1016/j.foodhyd.2020.106223

Green, A. R., Nissen, M. S., Kumar, G. N. M., Knowles, N. R., & Kang, C. H. (2013). Characterization of Solanum tuberosum multicystatin and the significance of core domains. *The Plant Cell, 25*(12), 5043–5052. https://doi.org/10.1105/tpc.113.121004

Han, S., Cui, F., McClements, D. J., Xu, X., Ma, C., Wang, Y., Liu, X., & Liu, F. (2022). Structural characterization and evaluation of interfacial properties of pea protein isolate-EGCG molecular complexes. *Foods, 11*(18), 2895. https://doi.org/10.3390/foods11182895

Hu, C., & Xiong, H. (2022). Structure, interfacial adsorption and emulsifying properties of potato protein isolate modified by chitosan. *Colloids and Surfaces A: Physicochemical and Engineering Aspects, 638*, Article 128314. https://doi.org/10.1016/j.colsurfa.2022.128314

Hu, C., Xiong, Z., Xiong, H., Chen, L., & Zhang, Z. (2021). Effects of dynamic high-pressure microfluidization treatment on the functional and structural properties of potato protein isolate and its complex with chitosan. *Food Research International, 140*, 109868. https://doi.org/10.1016/j.foodres.2020.109868

Hussain, A., Qayum, A., Xiuxiu, Z., Hao, X., Liu, L., Hussain, K., Wang, Y., & Li, X. (2021b). Improvement in bioactive, functional, structural and digestibility of potato protein and its fraction patatin via ultra-sonication. *LWT, 148*, Article 111747. https://doi.org/10.1016/j.lwt.2021.111747

Hussain, M., Qayum, A., Xiuxiu, Z., Liu, L., Hussain, K., Yue, P., … Li, X. (2021a). Potato protein: An emerging source of high quality and allergy free protein, and its possible future based products. *Food Research International, 148*, 110583. https://doi.org/10.1016/j.foodres.2021.110583

Ji, W., Yang, F., & Yang, M. (2022). Effect of change in pH, heat and ultrasound pre-treatments on binding interactions between quercetin and whey protein concentrate. *Food Chemistry, 384*, 132508. https://doi.org/10.1016/j.foodchem.2022.132508

Li, M., Ritzoulis, C., Du, Q., Liu, Y., Ding, Y., Liu, W., & Liu, J. (2021). Recent progress on protein-polyphenol complexes: Effect on stability and nutrients delivery of oil-in-water emulsion system. *Frontiers in Nutrition, 8*. https://doi.org/10.3389/fnut.2021.765589 [Review].

Jiao, B., Shi, A., Wang, Q., & Binks, B. P. (2018). High-internal-phase pickering emulsions stabilized solely by peanut-protein-isolate microgel particles with multiple potential applications. *Angewandte Chemie International Edition, 57*(30), 9274–9278. https://doi.org/10.1002/anie.201801350

Kew, B., Holmes, M., Stieger, M., & Sarkar, A.. (2021). Oral tribology, adsorption and rheology of alternative food proteins. *Food Hydrocolloids, 116*, 106636. https://doi.org/10.1016/j.foodhyd.2021.106636

Li, X., Hu, S., Rao, W., Ouyang, L., Zhu, S., Dai, T., … Zhou, J. (2023). Study on the interaction mechanism, physicochemical properties and application in oil-in-water emulsion of soy protein isolate and tannic acid. *Journal of Food Engineering, 357*, 111626. https://doi.org/10.1016/j.jfoodeng.2023.111626

Li, S., & McClements, D. J. (2023). Controlling textural attributes of plant-based emulsions using heteroaggregation of cationic and anionic potato protein-coated oil droplets. *Food Hydrocolloids, 145*, Article 109126. https://doi.org/10.1016/j.foodhyd.2023.109126

Liang, Q., Sun, X., Raza, H., Khan, M. A., Ma, H., & Ren, X. (2021). Fabrication and characterization of quercetin loaded casein phosphopeptides-chitosan composite nanoparticles by ultrasound treatment: Factor optimization, formation mechanism, physicochemical stability and antioxidant activity. *Ultrasonics Sonochemistry, 80*, Article 105830. https://doi.org/10.1016/j.ultsonch.2021.105830

Liao, L., McClements, D. J., Chen, X., Zhu, Y., Liu, Y., Liang, R., … Liu, W. (2022). Dietary proteins as excipient ingredients for improving the solubility, stability, and bioaccessibility of quercetin: Role of intermolecular interactions. *Food Research International, 161*, 111806. https://doi.org/10.1016/j.foodres.2022.111806

Liu, F., Ma, C., McClements, D. J., & Gao, Y. (2017). A comparative study of covalent and non-covalent interactions between zein and polyphenols in ethanol-water solution. *Food Hydrocolloids, 63*, 625–634. https://doi.org/10.1016/j.foodhyd.2016.09.041

Liu, J., Ghanizadeh, H., Li, X., Han, Z., Qiu, Y., Zhang, Y., … Wang, A. (2021). A study of the interaction, morphology, and structure in trypsin-epigallocatechin-3-gallate complexes. *Molecules, 26*(15), 4567. https://doi.org/10.3390/molecules26154567

Liu, Y., Qian, J., Li, J., Xing, M., Grierson, D., Sun, C., Xu, C., Li, X., & Chen, K. (2022). Hydroxylation decoration patterns of flavonoids in horticultural crops: Chemistry, bioactivity, and biosynthesis. *Horticulture Research, 9*. https://doi.org/10.1093/hr/uhab068

Ma, J. -J., Huang, X. -N., Yin, S. -W., Yu, Y.-G., & Yang, X. -Q. (2021). Bioavailability of quercetin in zein-based colloidal particles-stabilized Pickering emulsions investigated by the in vitro digestion coupled with Caco-2 cell monolayer model. *Food Chemistry, 360*, 130152. https://doi.org/10.1016/j.foodchem.2021.130152

Nimaming, N., Sadeghpour, A., Murray, B. S., & Sarkar, A. (2023). Hybrid particles for stabilization of food-grade Pickering emulsions: Fabrication principles and interfacial properties. *Trends in Food Science & Technology*. https://doi.org/10.1016/j.tifs.2023.06.034

Yi, C., Gan, C., Wen, Z., Fan, Y., & Wu, X. (2021). Development of pea protein and high methoxyl pectin colloidal particles stabilized high internal phase pickering emulsions for β-carotene protection and delivery. *Food Hydrocolloids, 113*, 106497. https://doi.org/10.1016/j.foodhyd.2020.106497. Article 106497.

Okeudo-Cogan, M., Yang, S., Murray, B. S., Ettelaie, R. E., Connell, S. D., Radford, S., Micklethwaite, S.-A., Benitez-Alfonso, Y., Yeshvekar, R., & Sarkar, A. (2024). Multivalent cations modulating microstructure and interactions of potato protein and fungal hyphae in a functional meat analogue. *Food Hydrocolloids, 149*, 109569. https://doi.org/10.1016/j.foodhyd.2023.109569

Pan, L., Chen, J., Fu, H., Wang, N., Zhou, J., Zhang, S., Lu, S., Song, J., Wang, Q., & Yan, H. (2023). Effects of fabrication of conjugates between different polyphenols and bovine bone proteins on their structural and functional properties. *Food Bioscience, 52*, Article 102375. https://doi.org/10.1016/j.fbio.2023.102375

Peng, D., Jin, W., Tang, C., Lu, Y., Wang, W., Li, J., & Li, B. (2018). Foaming and surface properties of gliadin nanoparticles: Influence of pH and heating temperature. *Food Hydrocolloids, 77*, 107–116. https://doi.org/10.1016/j.foodhyd.2017.09.026

Qin, X.-S., Luo, Z.-G., & Peng, X.-C. (2018a). Fabrication and characterization of quinoa protein nanoparticle-stabilized food-grade pickering emulsions with ultrasound treatment: Interfacial adsorption/arrangement properties. *Journal of Agricultural and Food Chemistry, 66*(17), 4449–4457. https://doi.org/10.1021/acs.jafc.8b00225

Qin, X.-S., Luo, Z.-G., Peng, X.-C., Lu, X.-X., & Zou, Y. X. (2018b). Fabrication and characterization of quinoa protein nanoparticle-stabilized food-grade pickering emulsions with ultrasound treatment: Effect of ionic strength on the freeze–thaw stability. *Journal of Agricultural and Food Chemistry, 66*(31), 8363–8370. https://doi.org/10.1021/acs.jafc.8b02407

Quan, T. H., Benjakul, S., Sae-leaw, T., Balange, A. K., & Maqsood, S. (2019). Protein–polyphenol conjugates: Antioxidant property, functionalities and their applications. *Trends in Food Science & Technology, 91*, 507–517. https://doi.org/10.1016/j.tifs.2019.07.049

Rydel, T. J.., Williams, J. M., Krieger, E., Moshiri, F., Stallings, W. C., Brown, S. M., … Alibhai, M. F. (2003). The crystal structure, mutagenesis, and activity studies reveal that patatin is a lipid acyl hydrolase with a ser-asp catalytic dyad. *Biochemistry, 42*(22), 6696–6708. https://doi.org/10.1021/bi027156r

Sarkar, A., & Dickinson, E. (2020). Sustainable food-grade Pickering emulsions stabilized by plant-based particles. *Current Opinion in Colloid & Interface Science, 49*, 69–81. https://doi.org/10.1016/j.cocis.2020.04.004

Schmidt, J. M., Damgaard, H., Greve-Poulsen, M., Larsen, L. B., & Hammershøj, M. (2018). Foam and emulsion properties of potato protein isolate and purified fractions. *Food Hydrocolloids, 74*, 367–378. https://doi.org/10.1016/j.foodhyd.2017.07.032

Schmidt, J. M., Damgaard, H., Greve-Poulsen, M., Sunds, A. V., Larsen, L. B., & Hammershøj, M. (2019). Gel properties of potato protein and the isolated fractions of patatins and protease inhibitors – impact of drying method, protein concentration, pH and ionic strength. *Food Hydrocolloids, 96*, 246–258. https://doi.org/10.1016/j.foodhyd.2019.05.022

Sui, X., Sun, H., Qi, B., Zhang, M., Yang, L., & Jiang, L. (2018). Functional and conformational changes to soy proteins accompanying anthocyanins: Focus on covalent and non-covalent interactions. *Food Chemistry, 245*, 871–878. https://doi.org/10.1016/j.foodchem.2017.11.090

Tavasoli, S., Liu, Q., & Jafari, S. M. (2022). Development of Pickering emulsions stabilized by hybrid biopolymeric particles/nanoparticles for nutraceutical delivery. *Food Hydrocolloids, 124*, 107280. https://doi.org/10.1016/j.foodhyd.2021.107280

van Koningsveld, Walstra, P., Voragen, A. G. J., Kuijpers, I. J., van Boekel, … Gruppen, H. (2006). Effects of protein composition and enzymatic activity on formation and properties of potato protein stabilized emulsions. *Journal of Agricultural and Food Chemistry, 54*(17), 6419–6427. https://doi.org/10.1021/jf061278z

Waglay, A., Karboune, S., & Alli, I. (2014). Potato protein isolates: Recovery and characterization of their properties. *Food Chemistry, 142*, 373–382. https://doi.org/10.1016/j.foodchem.2013.07.060

Wang, C., Guan, X., Sang, J., Zhou, J., Wang, C., Ngai, T., & Lin, W. (2023). General liquid vegetable oil structuring via high internal phase Pickering emulsion stabilized by soy protein isolate nanoparticles. *Journal of Food Engineering, 356*, 111595. https://doi.org/10.1016/j.jfoodeng.2023.111595

Zembyla, M., Murray, B. S., Radford, S. J., & Sarkar, A. (2019). Water-in-oil Pickering emulsions stabilized by an interfacial complex of water-insoluble polyphenol crystals and protein. *Journal of Colloid and Interface Science, 548*, 88–99. https://doi.org/10.1016/j.jcis.2019.04.010

Zembyla, M., Murray, B. S., & Sarkar. (2018). Water-in-oil pickering emulsions stabilized by water-insoluble polyphenol crystals. *Langmuir, 34*(34), 10001–10011. https://doi.org/10.1021/acs.langmuir.8b01438

Zhang, R., Belwal, T., Li, L., Lin, X., Xu, Y., & Luo, Z. (2020a). Recent advances in polysaccharides stabilized emulsions for encapsulation and delivery of bioactive food ingredients: A review. *Carbohydrate Polymers, 242*, Article 116388. https://doi.org/10.1016/j.carbpol.2020.116388

Zhang, S., Holmes, M., Ettelaie, R., & Sarkar, A. (2020b). Pea protein microgel particles as Pickering stabilisers of oil-in-water emulsions: Responsiveness to pH and ionic strength. *Food Hydrocolloids, 102*, Article 105583. https://doi.org/10.1016/j.foodhyd.2019.105583

Zhang, Q., Cheng, Z., Wang, Y., & Fu, L. (2021b). Dietary protein-phenolic interactions: Characterization, biochemical-physiological consequences, and potential food applications. *Critical Reviews in Food Science and Nutrition, 61*(21), 3589–3615. https://doi.org/10.1080/10408398.2020.1803199

Zhang, R., Cheng, L., Luo, L., Hemar, Y., & Yang, Z. (2021). Formation and characterisation of high-internal-phase emulsions stabilised by high-pressure homogenised quinoa protein isolate. *Colloids and Surfaces A: Physicochemical and Engineering Aspects, 631*, 127688. https://doi.org/10.1016/j.colsurfa.2021.127688

Zhang, S., Murray, B. S., Suriyachay, N., Holmes, M., Ettelaie, R., & Sarkar. (2021c). Synergistic interactions of plant protein microgels and cellulose nanocrystals at the interface and their inhibition of the gastric digestion of pickering emulsions. *Langmuir, 37*(2), 827–840. https://doi.org/10.1021/acs.langmuir.0c03148

Zheng, X., Ren, C., Wei, Y., Wang, J., Xu, X., Du, M., & Wu, C. (2023). Soy protein particles with enhanced anti-aggregation behaviors under various heating temperatures, pH, and ionic strengths. *Food Research International, 170*, 112924. https://doi.org/10.1016/j.foodres.2023.112924